Tribol Lett (2012) 47:195–202
DOI 10.1007/s11249-012-9978-8

ORIGINAL PAPER

Tribological Properties of Nanodiamond-Epoxy Composites

I. Neitzel · V. Mochalin · J.A. Bares · R.W. Carpick · A. Erdemir · Y. Gogotsi

Received: 21 December 2011 / Accepted: 6 May 2012 / Published online: 24 May 2012

Abstract Owing to its superior mechanical properties, nanodiamond (ND) holds great potential to improve tribological characteristics of composites. In this study, we report on the wear and dry friction of epoxy-ND composites prepared from as-received and aminated ND across the length scale range from macro to nano. Comparison of macroscale, microscale, and nanoscale frictional behavior shows that ND is highly effective in improving the wear resistance and friction coefficients of polymer matrices across the different length scales. Although with both types of ND wear resistance and friction coefficients of epoxy-ND composites were significantly improved, aminated ND outperformed as-received ND, which we account to the formation of a strong interface between aminated ND and the epoxy matrix. This study also shows that agglomerates within epoxy-ND composites containing 25 vol.% ND were able to wear an alumina counterbody, indicating very high hardness and Young's modulus of these agglomerates, that can eventually replace micron sized diamonds currently used in industrial abrasive applications.

Keywords Tribology · Nanodiamond · Epoxy · Nanocomposite · Friction · Wear

I. Neitzel · V. Mochalin · Y. Gogotsi (✉)
Department of Materials Science & Engineering, Drexel University, Philadelphia, PA 19104, USA
e-mail: gogotsi@drexel.edu

J.A.Bares · R.W.Carpick
Department of Mechanical Engineering & Applied Mechanics, University of Pennsylvania, Philadelphia, PA 19104, USA

A. Erdemir
Energy Systems Division, Argonne National Laboratory, Argonne, IL 60439, USA

1 Introduction

Wear resistant materials with low friction coefficients are of interest in many applications where surfaces come into contact with each other. Polymers are commonly used to reduce friction between two surfaces, e.g., as bearings between steel counterparts or as coatings in joint prostheses [1–4]. To improve their tribological performance and produce solid, self-lubricating materials, polymer composites with additives such as graphite, polyether ether ketone (PEEK), bronze, and alumina were proven to be effective, even replacing metals, commonly used in high performance wear applications [5, 6]. Further improvements in tribological properties are possible when macroscopic and nanoscopic fillers are combined [7]. Recently, it was shown that functionalized nanofillers can improve the wear resistance of thermosetting polymer matrices by up to 800 % [8–10].

Nanodiamond (ND) attracts much attention of the polymer-composite community. Having superior mechanical properties (Young's modulus 1,220 GPa, hardness 10 on the Mohs scale), a low friction coefficient [11], excellent thermal conductivity, unique electrical and optical properties [12], biocompatibility [13], ND combines an inert diamond core with a large accessible and reactive surface [14] in a particle of 5 nm or less in diameter. It has proven to be an excellent candidate for biomedical [15, 16], electrochemical [17], and composite applications [18–20]. Several studies on polymer-ND composites have shown that ND can be used to improve the mechanical properties of polymer matrices [19, 21]. To achieve these improvements, it is of outmost importance to adjust NDs' surface chemistry to the polymer. For example, hydrophobic ND obtained by functionalization using octadecylamine outperformed unmodified ND in a hydrophobic biodegradable

poly(L-lactic acid) matrix [18]. Aminated, hydrophilic ND (ND–NH_2) was used to covalently incorporate ND into an epoxy matrix resulting in high Young's moduli [22].

Tribological studies on polymer-ND composites are rare even though it is well known that in many environments single and polycrystalline diamond exhibits excellent performance in tribological applications, for example in the form of smooth CVD diamond coatings [23, 24]. Lee et al. [25] showed that ND can improve the macroscopic wear resistance of polytetrafluoroethylene (PTFE) films, while Voznyakovskii et al. [26] reported on improved tribological properties of polyurethane-ND composites. Also, in our previous study, we reported on a stiffened epoxy-ND composite (470 % increased Young's modulus and 300 % increased hardness) with a 40 % decreased friction coefficient due to the addition of 25 vol.% of as-received ND [27]. However, the tribological properties of composites with functionalized ND were not reported. In the present study, tribological properties of as-received and ND–NH_2-epoxy composites were measured using macroscale (pin-on-disk), microscale (nanoindentation) and nanoscale (AFM) techniques.

2 Materials and Methods

2.1 Materials

ND powder UD90 (NanoBlox, Inc. USA) with an average particle diameter of 5 nm characterized in [28] was used as received and after reaction with ethylenediamine (Sigma-Aldrich) resulting in aminated ND (ND–NH_2). Synthesis and characterization of ND–NH_2 is described elsewhere [22]. The epoxy system Epon828 (diglycidyl ether of bisphenol A; Hexicon, USA)-PACM (bis-*p*-aminocyclohexyl methane; Air Products, USA) was used in this study. The stoichiometry and resulting properties of this system are well known and are described elsewhere [29]. The predetermined amounts of Epon828, ND/ND–NH_2 were mixed and bath sonicated for 5 min in tetrahydrofuran (Fisher Scientific, 99.9 %, stabilized). The solutions were stirred in closed vials on a hot plate for 2 days at 50 °C, followed by opening the vials and solvent evaporation for 48 h at 50 °C. For ND concentrations below 12.5 vol.%, the composites were cured in 20-mm diameter aluminum molds for 2 h at 80 °C and 2 h at 165 °C following the standard curing procedure for the Epon828-PACM system after adding 28 pph (parts per hundred, i.e., 28 g per 100 g of Epon828) of the curing agent according to stoichiometry of this system [29]. Owing to the high viscosity of epoxy-ND samples with contents higher than 7.5 vol.% ND, resulting wet ND/ND–NH_2-Epon828 pastes were transferred into 5-mm (samples for nanoindentation) and 20-mm (samples for bulk wear tests) diameter hot pressing molds and the curing agent was added. After hand mixing in the mold, the pastes were pressed at a load of 4 tonnes for 2 h at 80 °C and 2 h at 165 °C following the curing procedure. All produced samples were polished for subsequent tribological tests using a Struers RotoPol-22 polishing machine after mounting them into Castolite; LECO, USA. The final polishing step was performed using an alumina polishing solution with an average particle size of 0.05 μm. All samples were cleaned in an ultrasonication bath before testing.

2.2 Wear and Friction Measurements

As previously reported, polymer-ND composites contain ND agglomerates, the sizes of which can be divided into the following three groups: 1st >0.6 μm; 2nd 0.2–0.5 μm; and 3rd ~100 nm [30]. Small agglomerates are contained within larger agglomerates and are individually dispersed in the polymer matrix itself. Macroscopic measurements with a pin-on-disk tester give average values for the entire composites, not distinguishing between locally changing properties. Nanoindentation probes properties on the μm scale, for example of single ND agglomerates. Furthermore, AFM measurements were used to measure properties of ~100 nm ND agglomerates, contained in larger assemblies, with nanometer resolution.

2.2.1 Pin-on-Disk

Macroscale tribological properties of test samples were evaluated in open air (35–40 % relative humidity) using a pin-on-disk tester (Nanovea tribometer) under a load of 5 N. Sintered alumina and AISI 52100 steel balls with diameters of 3/8″ were used as counterbodies. The testing time for the alumina counterbody was 45 min and it was 480 min for the steel counterbodies. Surfaces of the worn composites and the counterbodies were analyzed using an optical surface profilometer (KLA Tencor, MicroXAM). Line scans were performed using a non-contact MicroXAM profilometer. Friction coefficients were measured continuously at a rotation speed of 10 rpm over a 10-mm track diameter. Reported average friction coefficients were calculated from the data collected in the sliding distance ranges of ~0–6 m and ~9–14 m.

Friction forces were recorded continuously by a data acquisition system. Values of friction coefficients were automatically calculated and tabulated in data tables from which the friction coefficient versus distance diagrams were extracted. Using the Micro XAM non-contact profilometer, line scans of wear tracks and counterbodies were obtained and used to assess the wear damage and calculate surface roughness.

2.2.2 Nanoindentation

Microscale friction coefficients of epoxy-ND composites were measured using a Nanoindenter XP (MTS Corp.) using a 100-μm radius diamond indenter to minimize plastic deformation. Five measurements per sample were performed at a fixed vertical indenter displacement of 300 nm to insure a close to constant contact area over a sliding distance of 250 μm and an indenter velocity of 10 μm/s. Each sliding test was performed in a single forward pass of the indenter. Friction coefficients were calculated from the lateral and normal forces acting on the indenter. Reported friction coefficients are the average values of five measurements.

2.2.3 AFM

Nanoscale properties of unworn composites were characterized using an Agilent PicoPlus 5500 AFM. Before imaging, samples were rinsed with methanol and dried in dry nitrogen gas flow. A rectangular silicon cantilever (MikroMasch; San Jose, CA) with a normal stiffness of 0.54 N/m was used for contact mode imaging in ambient air. Topography and friction voltage were recorded for each contact mode scan. The normal cantilever stiffness was calibrated by the Sader method [31] and friction forces were calibrated by the wedge method [32, 33].

3 Results and Discussion

3.1 Macroscale Pin-on-Disk

3.1.1 Wear

Light micrographs of wear tracks induced by an alumina counterbody on neat (Fig. 1a) and 25 vol.% epoxy-ND (Fig. 1b) were captured. Wear tracks of composites containing 7.5 and 12.5 vol.% ND were not observable by light microscopy, indicating a significantly improved bulk wear resistance. At a ND concentration of 25 vol.% wear tracks became traceable again by dark field imaging (Fig. 1b). Abrasive wear resulting in "smearing" of the composite and extensive perpendicular cracks over inconsistent wear tracks further suggest a "stick–slip" motion of the alumina counterbody on this sample. Also, intact, up to 300-μm ND-epoxy agglomerates found within the wear tracks provide evidence of a significantly higher hardness of the agglomerates compared to the surrounding matrix. Profilometer scans of the alumina counterbody support this hypothesis showing significant damage after tests on epoxy-ND composites containing 12.5 vol.% ND (Fig. 1c). This damage of the counterbody can only be explained if we assume that ND-epoxy agglomerates have a hardness comparable or higher to that of alumina (up to 20 GPa) [34]. Interestingly, such severe damage of the counterbody was not observed for composites with higher or lower contents of ND.

To gain more information on the tribological performance of epoxy-ND composites, a softer steel counterbody was used at longer testing distances of 25 m. Topographical images and line scans of the wear tracks (Fig. 2a) and steel counter bodies (Fig. 2b) on neat epoxy and epoxy-ND/ND-NH_2 composites were produced by optical profilometry. For the neat epoxy sample, wear tracks and debris were observed, while the steel counterbody did not show any signs of damage. At a ND loading of 4 vol.%, steel counterbody and wear track line scans show almost no wear. ND loading of 7.5 vol.% ND further improves the wear resistance of the composites as topographical images and line scans show almost no removal of material. At the same time, the steel counterbody gets damaged, probably cut by ND agglomerates contained within the wear debris building up during testing. This effect becomes more pronounced when further increasing ND loadings to 12.5 vol.%. The damaged steel counterbody introduces deeper grooves into the composite,

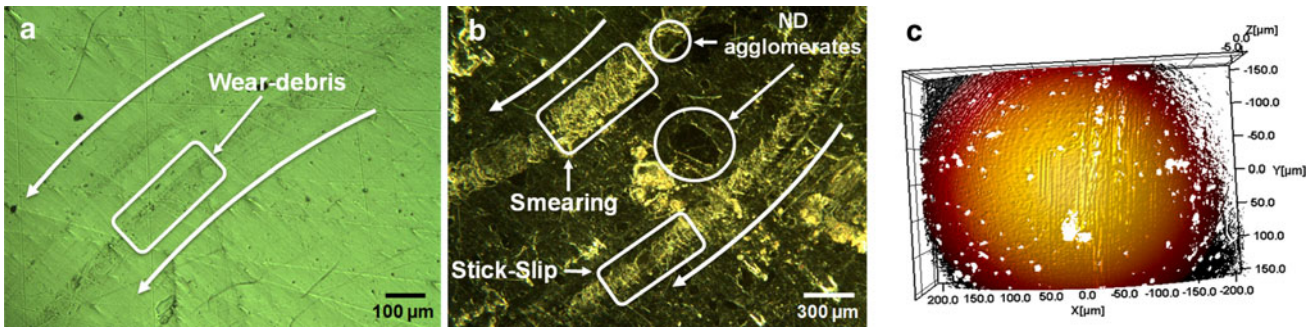

Fig. 1 **a** Bright field image of wear tracks on a neat epoxy sample. Continuous removal of material can be observed. **b** Dark field image of wear tracks on a 25 vol.% ND sample. Intact ND agglomerates within the wear tracks indicate a high resistance against wear. **c** 3D-Surface scan of an alumina counterbody after a wear test on a 12.5 vol.% ND-epoxy composite showing significant damage

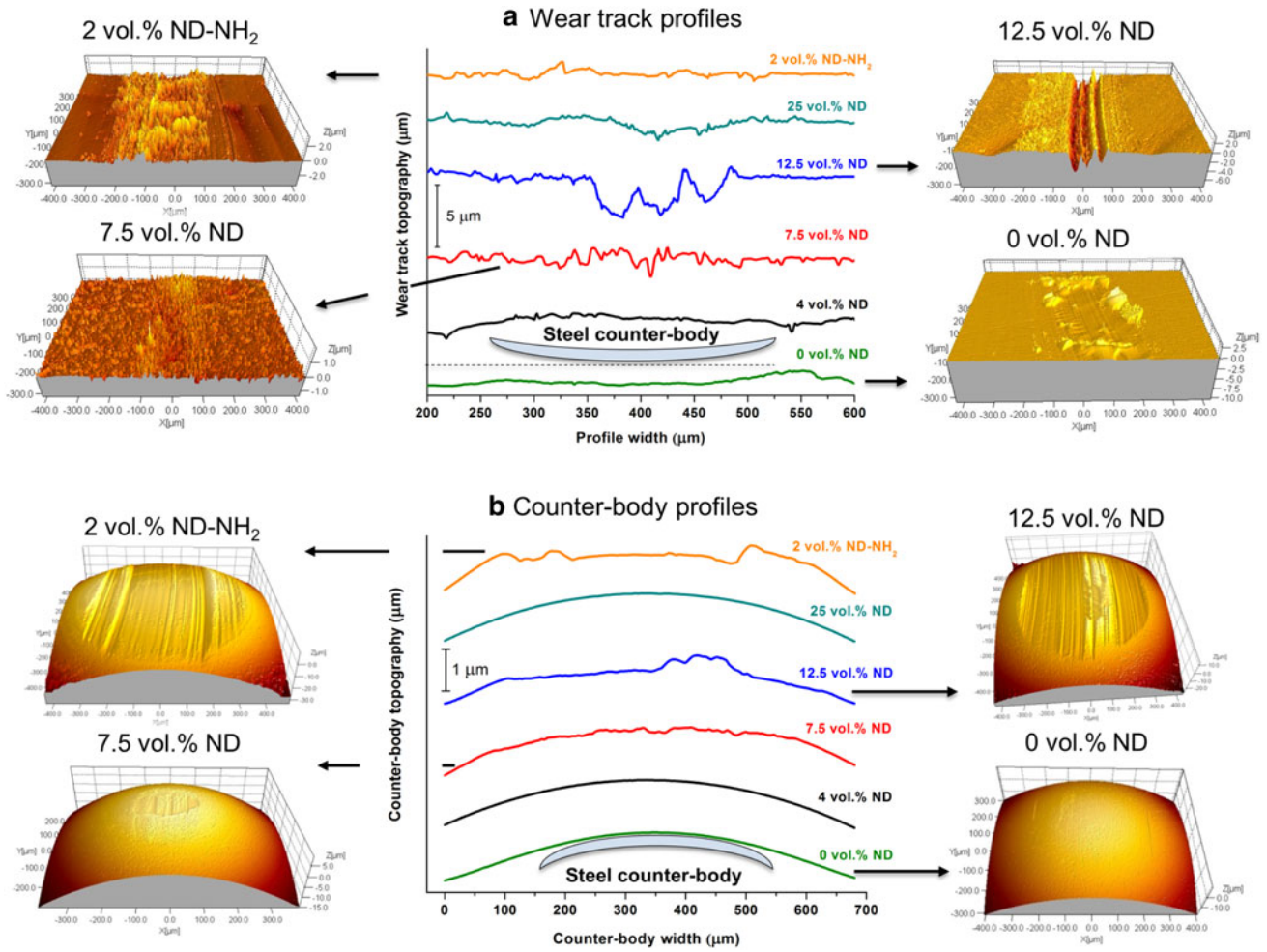

Fig. 2 **a** 3D-Profile and line scans of wear tracks on neat epoxy, epoxy-ND, and epoxy-ND–NH_2 composites. **b** 3D-Profile and line scans of the steel counter bodies after the tests

i.e., up to 3-µm deep. We suspect that ND agglomerates at ND contents below 25 vol.% get pulled out of the matrix damaging the counterbodies. However, at ND concentrations of 25 vol.%, the steel counterbody stays almost intact and less wear of the composite is measured. At this high concentration of ND, the composites can be thought of as a porous ND-body infiltrated by epoxy [27], explaining the reversed trend in the tribological behavior, observed for both steel and alumina counterbodies: the high wear resistance of these composites prevents plowing of the wear tracks, resulting in a smaller contact area and making ND agglomerate pull-out difficult. A previous study of PTFE-ND composites reported on the effect of agglomerate size on the wear performance of the composites. Smaller agglomerate size was found to decrease wear rate [35]. We assume that the same effect is taking place in epoxy-ND composites explaining the better performance of epoxy-ND composites containing 7.5 vol.% ND.

To understand the effect of surface functionalization of ND on the tribological performance of epoxy-ND composites, samples with 2 vol.% of ND–NH_2 were tested. Even at this low concentration of ND–NH_2, the wear resistance of the composites is significantly improved (almost no wear was observed; Fig. 2a). At the same time, the steel counterbody shows the most severe damage within this study (Fig. 2b) resulting in a rougher wear track (Fig. 2a). The strong interface between covalently incorporated ND–NH_2 particles and the epoxy matrix prevents pullout of ND–NH_2, which can explain the improved wear resistance. At the same time, the high hardness of ND causes the severe damage of the steel counter body.

3.1.2 Friction

Continuously recorded and averaged macroscale dry friction coefficients calculated from macroscopic pin-on-disk test data in the range of 0–6 and 9–14 m are shown in

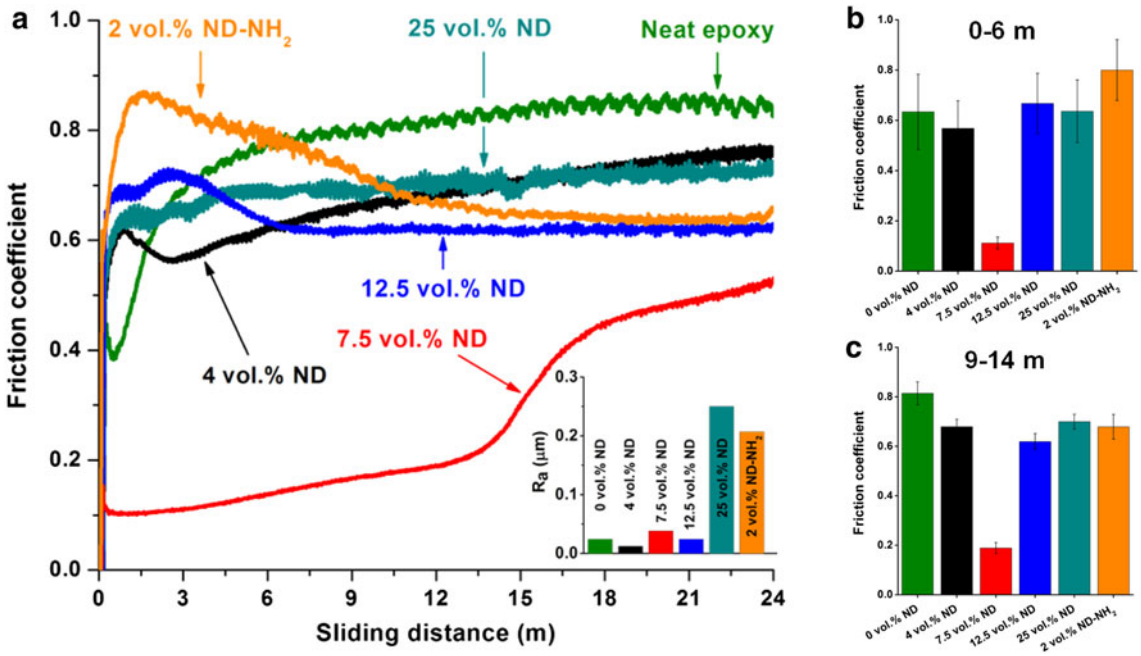

Fig. 3 **a** Development of friction coefficients over a testing distance of 24 m. Steel counter bodies were used for these tests. *Inset*: surface roughness R_a, measured before testing. **b** Averaged bulk friction coefficients in the range of 0–6 m and **c** 9–14 m

Fig. 3a–c. The stabilization of friction coefficients at longer testing times for neat epoxy and all epoxy-ND-NH_2 composites suggests plowing of the wear tracks resulting in an increased surface area. This hypothesis is confirmed by the significant decrease in standard deviations of averaged friction coefficients measured in the range of 9–14 m when compared to the initial ones in the range of 0–6 m: larger initial fluctuations in friction coefficients are related to the variation in topography before testing. When the test progresses (longer testing distance), the standard deviation of friction coefficients decreases due to the formation of wear tracks (Fig. 3b, c). This is confirmed by comparing the surface roughness (R_a) before testing (Fig. 3a, inset): due to the different responses to polishing of the neat epoxy and epoxy-ND composites, R_a values differ. Therefore, friction coefficients before plowing cannot be compared. However, after plowing of the wear tracks, smoothening the surface, friction coefficients can be fairly compared (9–14 m (Fig. 3c)). Friction coefficients decrease from 0.80 ± 0.05 for neat epoxy to 0.67 ± 0.03 for a 4 vol.% ND composite, slightly increasing over the testing distance (Fig. 3a, c). Addition of 7.5 vol.% ND to epoxy results in a four times lower friction coefficient of 0.19 ± 0.02, the largest decrease in bulk friction coefficient measured in this study (Fig. 3c). In contrast to the other composites, the initial friction coefficient for 7.5 vol.% ND is stable and has a remarkably low value of 0.1 ± 0.02, increasing at a sliding distance of about 13 m (Fig. 3a). The start of abrasive wear at 13 m might result from a weak interface between ND agglomerates and the epoxy matrix, leading to agglomerate pull-out. The friction coefficient of a composite containing 12.5 vol.% ND stabilizes at a value of 0.60 ± 0.03. A composite with 25 vol.% ND has a friction coefficient of 0.70 ± 0.03, nearly constant over the entire testing distance, indicating almost no plowing and thus a high wear resistance. The slightly higher friction coefficients for composites containing higher loadings of ND might originate from an uneven composite morphology even after plowing, where ND agglomerates stick out of the matrix, hindering the counterbody movement. The 25 vol.% ND composite has the highest surface roughness ($R_a = 0.25$ μm) prior to testing (Fig. 3a, inset).

Epoxy composites containing ND–NH_2 perform rather differently: The friction coefficient initially increases to 0.8 ± 0.1 and then decreases with sliding distance, stabilizing at a value of 0.68 ± 0.05. The high initial increase is in agreement with the observed severe damage of the steel counterbody and the higher surface roughness measured before testing, originating from the sample response to polishing. We account the improved performance at long testing times to a stronger interface between ND–NH_2 and epoxy, resulting from the covalent incorporation of ND–NH_2 into the epoxy matrix [22], improving the wear resistance of the composite.

3.2 Microscale Test Using Nanoindentation

To gain further insights into the friction behavior at the micrometer scale, nanoindentation sliding tests were performed. Averaged and continuously measured friction

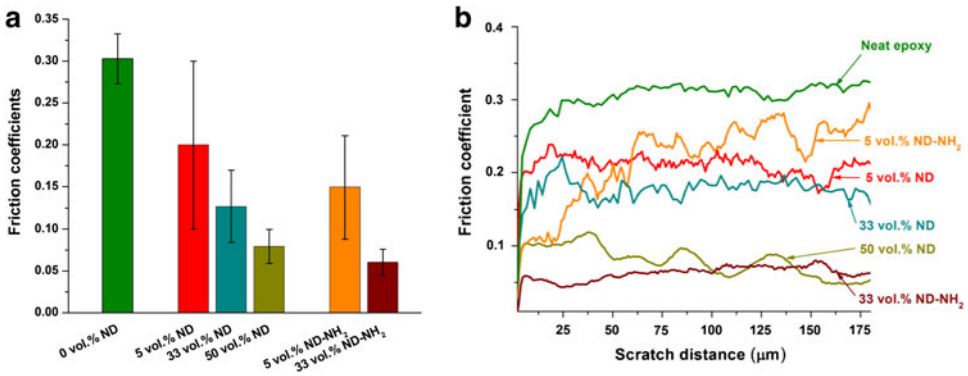

Fig. 4 **a** Averaged microscale friction coefficients. **b** Experimental curves (one out of five) measured using a diamond nanoindenter

coefficients are shown in Fig. 4a, b. With as-received ND, averaged microscale friction coefficients are significantly reduced from 0.30 ± 0.03 for neat epoxy to 0.2 ± 0.1 for the 5 vol.% ND composite. Further increases in ND contents to 33 and 50 vol.% result in decreased friction coefficients to 0.13 ± 0.04 and 0.08 ± 0.02, respectively. The low microscopic friction coefficients at high ND contents stand in contrast to the measured macroscopic friction coefficients, the latter increased at ND contents higher than 7.5 vol.%. This is an illustration of the difference between bulk and microscopic properties. The sliding length of the nanoindenter is only 250 μm in comparison to 24 m in macroscale tests. At these small length scales, it becomes possible to measure friction coefficients on single ND agglomerates, where ND concentration within ND agglomerates is high and constant. Furthermore, variations in the area of contact between macroscopic and microscopic measurements, resulting from the differences in indenter size and displacement, contribute to the observed differences. To investigate the influence of surface roughness on microscopic friction coefficients, data were recorded continuously and shown in Fig. 4b. According to these measurements, surface roughness does not seem to be the major mechanism for reducing friction coefficients of epoxy-ND composites since differences in surface roughness (fluctuations of friction coefficients) between neat and high concentration ND samples (33 and 50 vol.% ND/ND–NH_2) are similar, but friction coefficients for epoxy ND composites are reduced by a factor of six. These results further suggest that uniform ND dispersion is essential to optimize composite properties, minimizing surface roughness, and show the potential of ND for tribological applications.

The addition of 5 vol.% aminated ND–NH_2 results in a friction coefficient of 0.15 ± 0.06, being slightly lower than the values measured on composites prepared with as-received material. This effect becomes more pronounced at higher ND–NH_2 loadings: a 33 vol.% ND–NH_2 composite shows the lowest measured friction coefficient within this study, 0.06 ± 0.02 (Fig. 4a), being ~ 50 % less when compared to the composite produced with 33 vol.% of as-received ND (0.13 ± 0.04). This value is close to the one reported for pure carbide-derived carbon (0.2) [36] or diamond-like carbon films (0.05) [37].

3.3 Nanoscale Friction Using AFM

To understand reinforcing mechanisms of as-received ND and ND–NH_2 on the epoxy matrix, AFM measurements were performed. Topographical maps and friction forces on neat epoxy and epoxy-ND/ND–NH_2 composites containing 12.5 vol.% are compared in Fig. 5. A smooth topography

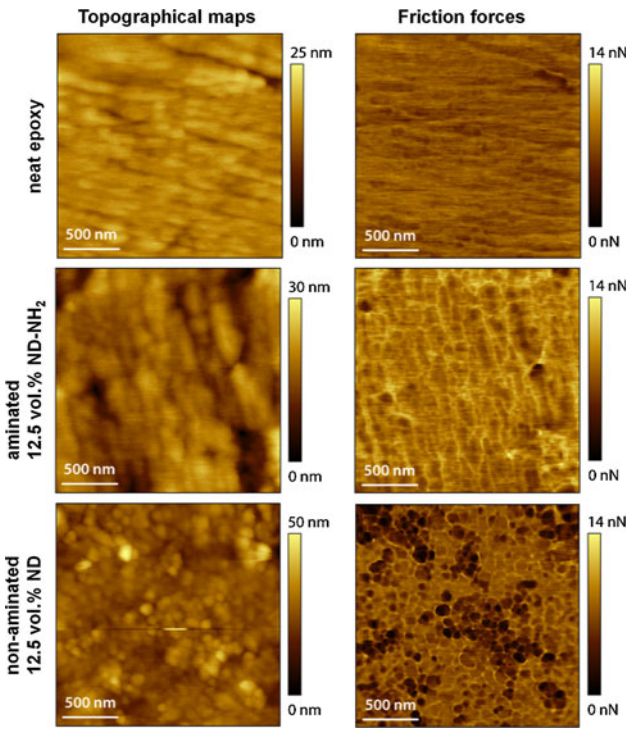

Fig. 5 Topographical and friction force maps recorded with AFM on neat epoxy and epoxy-ND composites containing 12.5 vol.% ND and ND–NH_2

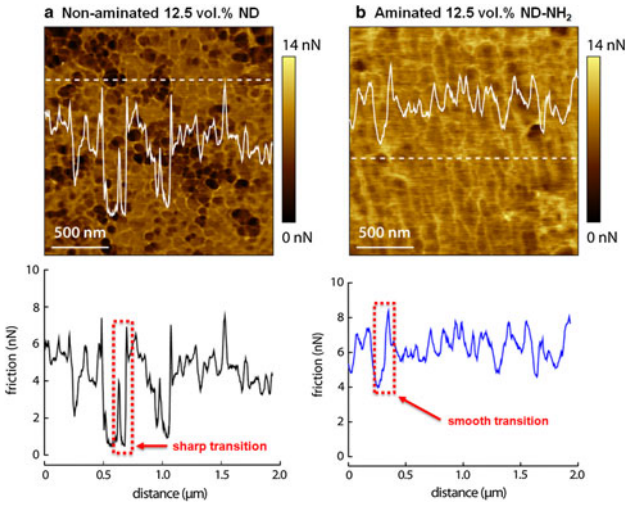

Fig. 6 AFM line scans of epoxy-ND composites containing **a** 12.5 vol.% ND and **b** 12.5 vol.% ND–NH_2. Composites containing as-received ND show sharp transitions in frictional forces. The usage of ND–NH_2 results in a strong interface between epoxy and ND–NH_2 and a smoother transition in frictional forces

and constant friction forces were measured on the neat epoxy sample. Scans performed on single ND agglomerates within epoxy-ND composites containing 12.5 vol.% ND show inconsistent behavior (notice the areas with higher and lower frictional forces in Fig. 5) revealing ND clusters with diameters of $\sim$100 nm within the epoxy-ND agglomerates. Friction forces are significantly lower than those recorded on the agglomerate matrix material and a sharp change in friction force is observed upon transition from either region (Fig. 6a). Thus, it is likely that weak interactions between ND clusters and the epoxy exist, being supported by topographical scans (Fig. 5, 12.5 vol.% ND), showing ND clusters sticking out of the sample surface. We suspect that the ND clusters can easily be pulled out of the epoxy matrix when a counterbody is sliding over the surface. Composites made with ND–NH_2 have a rather different structure: transitions between low and high friction force areas are smoother and have a lower amplitude (Fig. 6b). Also, ND–NH_2 clusters have smaller sizes of $\sim$50 nm (Fig. 5; 12.5 vol.% ND–NH_2) and suggest better integration into the epoxy matrix due to the covalent incorporation of ND–NH_2 [22].

4 Conclusion

Macroscale, microscale, and nanoscale measurements of the tribological properties of epoxy-ND composites have shown significant differences in the tribological behavior at the different length scales. The macroscale wear resistance of composites containing 4 and 7.5 vol.% ND was significantly improved over neat epoxy, as confirmed by light microscopy and optical profilometer scans of wear tracks and counterbodies after macroscopic pin-on-disk tests. Average friction coefficients were reduced by a factor 4 due to the addition of 7.5 vol.% ND, where the lowest friction coefficient of 0.1 ± 0.02, an eight times decrease, was measured. Also, abrasive wear on epoxy-ND composites containing 25 vol.% ND was observed, while composites containing 12.5 vol.% ND severely damaged the alumina counterbody, indicating highest hardness values of epoxy-ND agglomerates. Thus, epoxy-ND agglomerates have the potential to replace micron-sized diamonds that are currently used in industrial applications for sawing, grinding, and polishing. Composites produced with aminated ND outperformed composites manufactured with non-aminated ND. Epoxy-ND–NH_2 composites containing 33 vol.% ND–NH_2 have a friction coefficient of 0.08 ± 0.02 in nanoindentation sliding tests, the lowest value measured in this study, coming close to values reported for carbide-derived or diamond-like films. AFM scans on epoxy-ND agglomerates revealed ND clusters of $\sim$100 nm in size having the lowest friction coefficients, explaining the observed decreases in both macro- and microscale friction coefficients. These scans suggest covalent incorporation of ND–NH_2 particles that might be responsible for the better performance of ND–NH_2-epoxy composites.

Acknowledgments Centralized Research Facilities at Drexel University provided access to the NanoIndenter XP and optical light microscope used in this work. AFM measurements were performed at the Nano-Bio Interface Center at the University of Pennsylvania. Macroscopic tribological properties were measured at the Argonne National Laboratory supported by the U.S. Department of Energy, Office of Energy Efficiency and Renewable Energy, under Contract No. DE-AC02-06CH11357. The work at Drexel University was supported by NSF grant CMMI-0927963.

References

1. Klein, J.: Shear, friction, and lubrication forces between polymer-bearing surfaces. Annu. Rev. Mater. Sci. **26**, 581–612 (1996)
2. Lancaster, J.K.: Polymer-based bearing materials: the role of fillers and fibre reinforcement. Tribology **5**, 249–255 (1972)
3. Rehbein, P., Wallaschek, J.: Friction and wear behaviour of polymer/steel and alumina/alumina under high-frequency fretting conditions. Wear **216**, 97–105 (1998)
4. Widmer, M.R., Heuberger, M., Vörös, J., Spencer, N.D.: Influence of polymer surface chemistry on frictional properties under protein-lubrication conditions: implications for hip-implant design. Tribol. Lett. **10**, 111–116 (2001)
5. Friedrich, K., Zhang, Z., Schlarb, A.K.: Effects of various fillers on the sliding wear of polymer composites. Compos. Sci. Technol. **65**, 2329–2343 (2005)
6. Donnet, C., Erdemir, A.: Historical developments and new trends in tribological and solid lubricant coatings. Surf. Coat. Technol. **180**, 76–84 (2004)

7. Chang, L., Zhang, Z., Ye, L., Friedrich, K.: Tribological properties of high temperature resistant polymer composites with fine particles. Tribol. Int. **40**, 1170–1178 (2007)
8. Chang, L., Zhang, Z., Breidt, C., Friedrich, K.: Tribological properties of epoxy nanocomposites: I. Enhancement of the wear resistance by nano-TiO_2 particles. Wear **258**, 141–148 (2005)
9. Zhang, Z., Breidt, C., Chang, L., Haupert, F., Friedrich, K.: Enhancement of the wear resistance of epoxy: short carbon fibre, graphite, PTFE and nano-TiO_2. Compos. A Appl. Sci. Manuf. **35**, 1385–1392 (2004)
10. Burris, D.L., Zhao, S., Duncan, R., Lowitz, J., Perry, S.S., Schadler, L.S., Sawyer, W.G.: A route to wear resistant PTFE via trace loadings of functionalized nanofillers. Wear **267**, 653–660 (2009)
11. Robertson, J.: Properties of diamond-like carbon. Surf. Coat. Technol. **50**, 185–203 (1992)
12. Mochalin, V.N., Shenderova, O., Ho, D., Gogotsi, Y.: The properties and applications of nanodiamonds. Nat. Nanotechnol. **7**, 11–23 (2012)
13. Schrand, A.M., Johnson, J., Dai, L., Hussain, S.M., Schlager, J.J., Zhu, L., Hong, Y., Ōsawa, E.: Cytotoxicity and genotoxicity of carbon nanomaterials. In: Webster, T.J. (ed.) Safety of Nanoparticles: From Manufacturing to Clinical Applications, pp. 1–29. Springer, New York (2009)
14. Osswald, S., Yushin, G., Mochalin, V., Kucheyev, S.O., Gogotsi, Y.: Control of sp^2/sp^3 carbon ratio and surface chemistry of nanodiamond powders by selective oxidation in air. J. Am. Chem. Soc. **128**, 11635–11642 (2006)
15. Khabashesku, V.N., Margrave, J.L., Barrera, E.V.: Functionalized carbon nanotubes and nanodiamonds for engineering and biomedical applications. Diam. Relat. Mater. **14**, 859–866 (2005)
16. Lam, R., Chen, M., Pierstorff, E., Huang, H., Osawa, E., Ho, D.: Nanodiamond-embedded microfilm devices for localized chemotherapeutic elution. ACS Nano **2**, 2095–2102 (2008)
17. Portet, C., Yushin, G., Gogotsi, Y.: Electrochemical performance of carbon onions, nanodiamonds, carbon black and multiwalled nanotubes in electrical double layer capacitors. Carbon **45**, 2511–2518 (2007)
18. Zhang, Q., Mochalin, V.N., Neitzel, I., Knoke, I.Y., Han, J., Klug, C.A., Zhou, J.G., Lelkes, P.I., Gogotsi, Y.: Fluorescent PLLA-nanodiamond composites for bone tissue engineering. Biomaterials **32**, 87–94 (2011)
19. Behler, K.D., Stravato, A., Mochalin, V., Korneva, G., Yushin, G., Gogotsi, Y.: Nanodiamond-polymer composite fibers and coatings. ACS Nano **3**, 363–369 (2009)
20. Stravato, A., Knight, R., Mochalin, V., Picardi, S.C.: HVOF-sprayed nylon-11+ nanodiamond composite coatings: production & characterization. J. Therm. Spray Technol. **17**, 812–817 (2008)
21. Shenderova, O., Tyler, T., Cunningham, G., Ray, M., Walsh, J., Casulli, M., Hens, S., McGuire, G., Kuznetsov, V., Lipa, S.: Nanodiamond and onion-like carbon polymer nanocomposites. Diam. Relat. Mater. **16**, 1213–1217 (2007)
22. Mochalin, V.N., Neitzel, I., Etzold, B.J.M., Peterson, A., Palmese, G., Gogotsi, Y.: Covalent incorporation of aminated nanodiamond into an epoxy polymer network. ACS Nano **5**, 7494–7502 (2011)
23. Grill, A.: Tribology of diamond like carbon and related materials: an updated review. Surf. Coat. Technol. **94**, 507–513 (1997)
24. Konicek, A., Grierson, D., Gilbert, P., Sawyer, W., Sumant, A., Carpick, R.: Origin of ultralow friction and wear in ultrananocrystalline diamond. Phys. Rev. Lett. **100**, 235502 (2008)
25. Lee, J.-Y., Lim, D.-S.: Tribological behavior of PTFE film with nanodiamond. Surf. Coat. Technol. **188**, 534–538 (2004)
26. Voznyakovskii, A., Ginzburg, B., Rashidov, D., Tochil'nikov, D., Tuichiev, S.: Structure, mechanical, and tribological characteristics of polyurethane modified with nanodiamonds. Polym. Sci. Ser. A **52**, 1044–1050 (2010)
27. Neitzel, I., Mochalin, V., Knoke, I., Palmese, G.R., Gogotsi, Y.: Mechanical properties of epoxy composites with high contents of nanodiamond. Compos. Sci. Technol. **71**, 710–716 (2011)
28. Mochalin, V., Osswald, S., Gogotsi, Y.: Contribution of functional groups to the Raman spectrum of nanodiamond powders. Chem. Mater. **21**, 273–279 (2009)
29. Palmese, G.R., McCullough, R.L.: Effect of epoxy-amine stoichiometry on cured resin material properties. J. Appl. Polym. Sci. **46**, 1863–1873 (1992)
30. Bershtein, V., Karabanova, L., Sukhanova, T., Yakushev, P., Egorova, L., Lutsyk, E., Svyatyna, A., Vylegzhanina, M.: Peculiar dynamics and elastic properties of hybrid semi-interpenetrating polymer network–3-D diamond nanocomposites. Polymer **49**, 836–842 (2008)
31. Sader, J.E., Chon, J.W.M., Mulvaney, P.: Calibration of rectangular atomic force microscope cantilevers. Rev. Sci. Instrum. **70**, 3967–3969 (1999)
32. Ogletree, D.F., Carpick, R.W., Salmeron, M.: Calibration of frictional forces in atomic force microscopy. Rev. Sci. Instrum. **67**, 3298–3306 (1996)
33. Varenberg, M., Etsion, I., Halperin, G.: An improved wedge calibration method for lateral force in atomic force microscopy. Rev. Sci. Instrum. **74**, 3362–3367 (2003)
34. Shen, Z., Johnsson, M., Zhao, Z., Nygren, M.: Spark plasma sintering of alumina. J. Am. Ceram. Soc. **85**, 1921–1927 (2002)
35. Lim, D.P., Lee, J.Y., Lim, D.S., Ahn, S.G., Lyo, I.W.: Effect of reinforcement particle size on the tribological properties of nanodiamond filled polytetrafluoroethylene based coating. J. Nanosci. Nanotechnol. **9**, 4197–4201 (2009)
36. Carroll, B., Gogotsi, Y., Kovalchenko, A., Erdemir, A., McNallan, M.J.: Effect of humidity on the tribological properties of carbide-derived carbon (CDC) films on silicon carbide. Tribol. Lett. **15**, 51–55 (2003)
37. Liu, Y., Erdemir, A., Meletis, E.I.: A study of the wear mechanism of diamond-like carbon films. Surf. Coat. Technol. **82**, 48–56 (1996)